

Enhanced Replication of Highly Pathogenic Influenza A(H7N9) Virus in Humans

Seiya Yamayoshi,¹ Maki Kiso, Atsuhiko Yasuhara, Mutsumi Ito, Yuelong Shu, Yoshihiro Kawaoka¹

To clarify the threat posed by emergence of highly pathogenic influenza A(H7N9) virus infection among humans, we characterized the viral polymerase complex. Polymerase basic 2–482R, polymerase basic 2–588V, and polymerase acidic–497R individually or additively enhanced virus polymerase activity, indicating that multiple replication-enhancing mutations in 1 isolate may contribute to virulence.

Highly pathogenic influenza A(H7N9) virus has infected humans every influenza season since 2013; the fifth epidemic wave occurred during the 2016–17 season (1,2). Since 2013, a total of 1,565 laboratory-confirmed human cases and 612 related deaths have been reported (http://www.who.int/influenza/human_animal_interface/Influenza_Summary_IRA_HA_interface_12_07_2017.pdf?ua=1). During the fifth wave, H7N9 viruses possessing hemagglutinin with multibasic amino acids at the cleavage site were isolated from birds and humans (2–4). H7N9 isolates from humans possessed hemagglutinin with a preference for human-type receptors and neuraminidase with inhibitor resistance (4,5); one of those isolates transmitted among ferrets via respiratory droplets (6). Emergence of highly pathogenic H7N9 viruses with such properties is a serious threat to public health. Full comprehension of the extent of this threat requires detailed characterization of these viruses.

The Study

We attempted to identify the replication-enhancing amino acids in the polymerase complex of H7N9 virus A/Guangdong/17SF003/2016 (GD), which was isolated from the first reported H7N9-infected patient (3,5) and harbors polymerase basic (PB) 2 with 271T, 588V, 591Q, 627E, and 701D. Amino acids at these positions are known to alter viral polymerase activity in mammalian and avian cells at different temperatures (7–11).

Author affiliations: University of Tokyo, Tokyo, Japan (S. Yamayoshi, M. Kiso, A. Yasuhara, M. Ito, Y. Kawaoka); Sun Yat-Sen University, Shenzhen, China (Y. Shu); Chinese Centers for Disease Control and Prevention, Beijing, China (Y. Shu); University of Wisconsin–Madison, Madison, Wisconsin, USA, and Japan Science and Technology Agency, Saitama, Japan (Y. Kawaoka)

We compared the viral polymerase activity of wild-type GD with that of A/Anhui/1/2013(H7N9) virus (AN) in human A549 cells at 33°C or 37°C (temperatures of the human upper and lower respiratory tract) and in chicken DF-1 cells at 39°C (body temperature of birds). Although both viruses exhibited comparable activity in DF-1 cells, AN activity was higher than GD activity in A549 cells at both temperatures because wild-type AN/PB2 acquired polymerase activity-enhancing K at position 627 of PB2 during replication in the infected human (8). We therefore tested AN/PB2-627E, which possesses an avian ancestral amino acid in PB2-627, and AN/PB2-627E-701N, which possesses polymerase-enhancing PB2-701N (8). In human A549 cells, wild-type GD showed viral polymerase activity comparable to that of AN/PB2-627E-701N (online Technical Appendix Figure 1, panel A, <https://wwwnc.cdc.gov/EID/article/24/4/17-1509-Techapp1.pdf>). These results indicate that the viral polymerase activity of wild-type GD in mammalian cells has increased more than that of virus bearing avian-like ancestral AN/PB2–627E.

To determine which component of the viral replication complex (PB2, PB1, polymerase acidic [PA], or nucleoprotein) contributes to the activity of the GD polymerase complex, we tested the polymerase activity of GD replication complexes in which we had replaced each viral protein with its AN/PB2-627E counterpart. We found that the viral polymerase activity in A549 cells was remarkably decreased by AN/PB2-627E and moderately decreased by AN-PA (online Technical Appendix Figure 1, panel B). These results suggest that the PB2 and the PA of GD are involved in the relatively high polymerase activity of the GD replication complex.

When we compared the amino acid sequences of GD-PB2 and GD-PA with those of AN/PB2-627E and AN-PA, we found 8 and 6 differences, respectively (Table 1). To identify which substitutions contributed to the enhanced polymerase activity, we constructed a series of plasmids encoding GD-PB2 or GD-PA harboring single substitutions and examined polymerase activity. Of the 8 PB2 mutants, GD/PB2-482K and GD/PB2-588A drastically reduced viral polymerase activity in A549 cells, although this activity was slightly higher than that of AN/PB2-627E (Figure 1, panel A). Therefore, we tested the viral polymerase activity of GD-PB2 possessing both mutations (GD/PB2-482K-588A) and found a further decrease in the double mutant. Of the 6 PA mutants, GD/PA-497K showed reduced

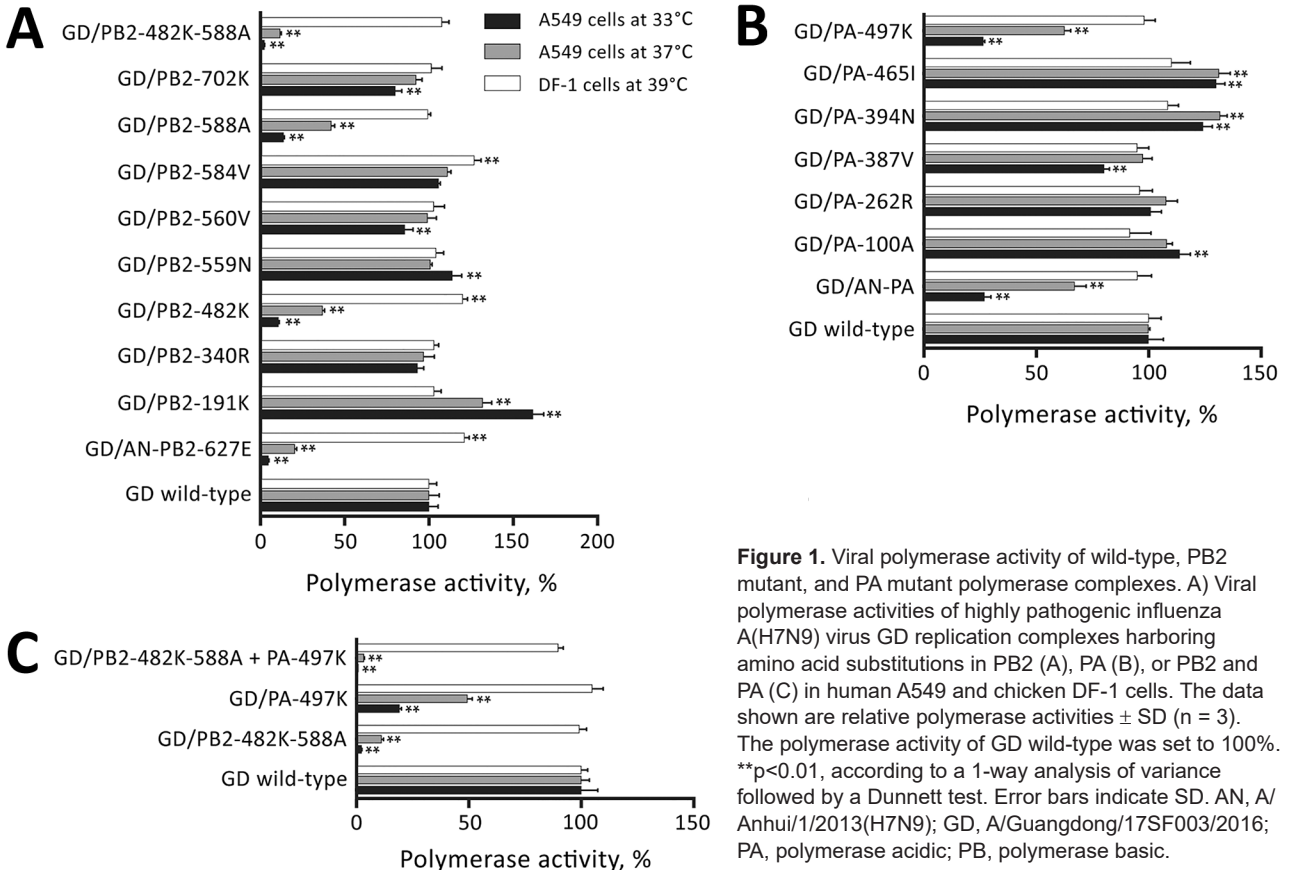
¹These senior authors contributed equally to this article.

Table 1. Amino acid differences between PB2 and PA in 2 influenza A(H7N9) viruses*

Virus	PB2								PA					
	191	340	482	559	560	584	588	702	100	262	387	394	465	497
GD wild-type	E	K	R	T	I	I	V	R	V	K	I	D	V	R
AN/PB2-627E†	K	R	K	N	V	V	A	K	A	R	V	N	I	K

*AN, A/Anhui/1/2013(H7N9); GD, A/Guangdong/17SF003/2016; PA, polymerase acidic; PB, polymerase basic.

†This mutant possessed a K to E substitution at position 627 of PB2, but the other residues of PB2 and PA were identical to those of wild-type AN.

**Figure 1.** Viral polymerase activity of wild-type, PB2 mutant, and PA mutant polymerase complexes. A) Viral polymerase activities of highly pathogenic influenza A(H7N9) virus GD replication complexes harboring amino acid substitutions in PB2 (A), PA (B), or PB2 and PA (C) in human A549 and chicken DF-1 cells. The data shown are relative polymerase activities \pm SD ($n = 3$). The polymerase activity of GD wild-type was set to 100%. ** $p < 0.01$, according to a 1-way analysis of variance followed by a Dunnett test. Error bars indicate SD. AN, A/Anhui/1/2013(H7N9); GD, A/Guangdong/17SF003/2016; PA, polymerase acidic; PB, polymerase basic.

viral polymerase activity in A549 cells (Figure 1, panel B). Compared with GD/PB2-482K-588A or GD/PA-497K alone, the polymerase activity of GD/PB2-482K-588A plus GD/PA-497K was further reduced (Figure 1, panel C). Collectively, these data demonstrate that PB-482R, PB2-588V, and PA-497R play crucial roles in the enhanced activity of the GD polymerase complex.

To examine the role of these amino acids on virus growth in human cells, we prepared wild-type and mutant viruses in the GD background by using reverse genetics. GD/PB2-482K and GD/PB2-588A viruses replicated less efficiently than wild-type GD virus in A549 cells (online Technical Appendix Figure 2, panels A, B). Replication of GD/PB2-482K-588A and GD/PB2-482K-588A+PA-497K

Table 2. Titers of influenza A(H7N9) GD virus in organs of experimentally infected mice*

Virus	Postinfection day 3, mean log ₁₀ PFU \pm SD/g			Postinfection day 6, mean log ₁₀ PFU \pm SD/g		
	Lung	NT	Brain	Lung	NT	Brain
GD wild-type	5.7 \pm 0.2	4.2 \pm 0.8	ND	5.8 \pm 0.4	5.9 \pm 0.7	3.2
GD/PB2-482K	ND, $p < 0.01$	ND, $p < 0.01$	ND	3.0, 3.4, $p < 0.01$	2.6 \pm 0.4, $p < 0.05$	ND
GD/PB2-588A	3.3 \pm 0.6, $p < 0.01$	3.1, $p < 0.01$	ND	4.6 \pm 0.8	4.4 \pm 2.5	ND
GD/PB2-482K-588A	ND, $p < 0.01$	ND, $p < 0.01$	ND	3.1 \pm 0.3, $p < 0.05$	ND, $p < 0.01$	ND
GD/PA-497K	5.1 \pm 0.2, $p < 0.05$	2.9 \pm 1.0	ND	4.6 \pm 1.0	5.8 \pm 0.4	ND
GD/PB2-482K-588A+PA-497K	ND, $p < 0.01$	ND, $p < 0.01$	ND	2.2, 2.7, $p < 0.01$	ND, $p < 0.01$	ND

*BALB/c mice were intranasally inoculated with 10^2 PFU of virus (in 50 μ L). Three animals per group were euthanized on postinfection days 3 and 6.Statistically significant differences compared with GD wild-type-infected mice were determined by use of a 1-way analysis of variance followed by a Dunnett test. GD, A/Guangdong/17SF003/2016; ND, virus not detected (detection limit ≈ 2 log₁₀ PFU/g); NT, nasal turbinates; PA, polymerase acidic; PB, polymerase basic.

viruses was less efficient than that of GD/PB2-482K and GD/PB2-588A viruses. GD/PA-497K virus showed growth comparable to that of the wild-type GD virus. In DF-1 cells, all tested viruses produced similar growth curves (online Technical Appendix Figure 2, panel C). These results indicate that PB2-482R and PB2-588V play a central role in enhancing virus replication in mammalian cells.

To assess the role of these amino acids *in vivo*, we compared virus titers in the lungs, nasal turbinates, and brains of mice infected intranasally with 10^2 PFU of each virus. On day 3 after infection, we did not detect GD/PB2-482K, GD/PB2-482K-588A, or GD/PB2-482K-588A+PA-497K viruses in the lungs or turbinates (Table 2). Replication of GD/PB2-588A or GD/PA-497K virus was significantly

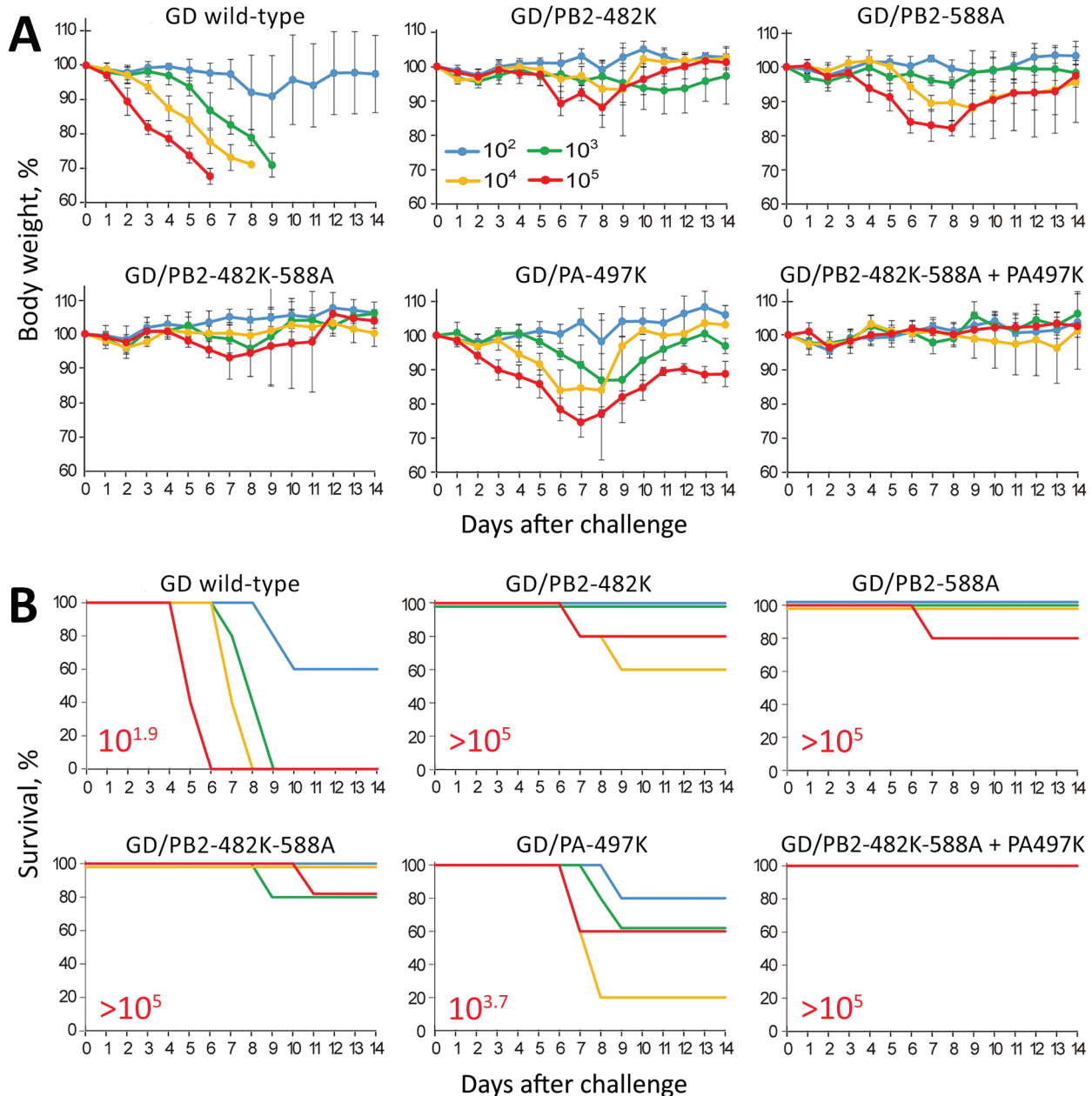


Figure 2. Virulence of wild-type and mutant highly pathogenic influenza A(H7N9) virus GD viruses in mice. Five mice per group were intranasally inoculated with 10^2 , 10^3 , 10^4 , or 10^5 PFU (each in 50 μ L) of the indicated viruses. Body weight (A) and survival (B) were monitored daily for 14 days. A) The values represent the average body weight \pm SD compared with the baseline weight from 5 mice. Two-way analysis of variance followed by a Dunnett test revealed that the body weight loss of mice infected with each mutant virus at any dose was significantly reduced compared with that of mice infected with GD wild-type virus ($p < 0.01$). B) The 50% lethal doses for mice (in red) were calculated according to the Spearman-Kärber method. Error bars indicate SD. GD, A/Guangdong/17SF003/2016; PA, polymerase acidic; PB, polymerase basic.

decreased in the lungs and slightly decreased in the turbinates. On day 6 after infection, we found similar trends to those observed on day 3. Wild-type GD virus was detected in the brain of 1 of 3 mice.

Next, we evaluated virus pathogenicity in mice infected with 10^2 – 10^5 PFU of each virus by monitoring changes in body weight. When inoculated with wild-type GD virus, almost all mice had to be euthanized, resulting in a 50% mouse lethal dose (MLD_{50}) of $10^{1.9}$ PFU (Figure 2, panels A and B). Transient or severe weight loss was caused by GD/PB2-482K, GD/PB2-588A, and GD/PB2-482K-588A in 1–3 of 20 euthanized mice and by GD/PA-497K viruses in 9 of 20 euthanized mice; MLD_{50} values were higher than those for wild-type GD virus. The GD/PB2-482K-588A+PA-497K virus did not affect body weight ($MLD_{50} > 10^5$ PFU). Virulence of GD/PB2-588A in mice was comparable to that of GD/PB2-482K and GD/PB2-482K-588A, although GD/PB2-588A replicated better in the lungs and turbinates than GD/PB2-482K and GD/PB2-482K-588A (Table 2); however, the levels of GD/PB2-588A replication in mice were lower than those of wild-type GD, resulting in reduced pathogenicity in mice. These results demonstrate that PB2-482R and PB2-588V contribute to high virulence in mice and that PA-497R is also involved.

Conclusions

We demonstrated that PB2-482R, PB2-588V, and PA-497R contribute to the enhanced polymerase activity of highly pathogenic H7N9 virus. These mutations additively increase viral polymerase activity and pathogenicity. PB2-482R is present in 0.79% (7/884) of human-derived H7N9 viruses, PB2-588V in 16.6% (147/883), and PA-497R in 0.81% (7/862) (online Technical Appendix Table). Of 31 highly pathogenic H7N9 viruses isolated from humans, 5 (16.1%) possessed PB2-482R and PA-497R, 12 (38.7%) PB2-627K, and 10 (32.3%) PB2-588V (online Technical Appendix Figure 3, panel A). Although conventional replication-enhancing amino acids (PB2-591R, PB2-627K, and PB2-701N) rarely coexist in 1 PB2 molecule, PB2-588V clearly permits acquisition of additional mutations, such as PB2-482R and PB2-627K (12). These double substitutions could have an additive effect on virulence enhancement, as also shown previously (9), suggesting that in mammalian hosts, these double-mutant viruses may be fitter than single-mutant viruses. Therefore, future H7N9 virus surveillance studies should take into consideration single markers and combinations of markers.

PB2-482R was located in 1 of 2 nuclear localization signals spanning amino acids 449 to 495 (13) within the cap-binding domain of the influenza A virus polymerase complex (online Technical Appendix Figure 3, panel B).

PB2-588V was located near PB2-627K in the 627 domain. PA-497R was located at 1 of 2 binding sites for transcriptional activator hCLE (14) but was not exposed on the protein surface. PB2-588V is probably involved in ANP32A-dependent high polymerase activity in mammalian hosts (15), and the role of PB2-482R might differ from that of other polymerase-enhancing amino acids in PB2.

Acknowledgments

We thank Kohei Oishi for assistance with experiments and Susan Watson for editing the manuscript.

This work was supported by the Japan Initiative for Global Research Network on Infectious Diseases from the Japan Agency for Medical Research and Development (AMED); Leading Advanced Projects for Medical Innovation from AMED; the e-ASIA Joint Research Program from AMED; a Grant-in-Aid for Scientific Research on Innovative Areas from the Ministry of Education, Culture, Science, Sports, and Technology of Japan (nos. 16H06429, 16K21723, and 16H06434); and the Center for Research on Influenza Pathogenesis funded by US National Institutes of Health, National Institute of Allergy and Infectious Diseases contract no. HHSN272201400008C.

Y.K. has received speaker's honoraria from Toyama Chemical and Astellas Inc., and grant support from Chugai Pharmaceuticals, Daiichi Sankyo Pharmaceutical, Toyama Chemical, Tauns Laboratories, Inc., Tsumura & Co., and Denka Seiken Co., Ltd. Y.K. is a co-founder of FluGen.

About the Author

Dr. Yamayoshi is project associate professor of Division of Virology, Institute of Medical Science, University of Tokyo. His research interests are virus–host interactions at the community, individual, cellular, and molecular levels.

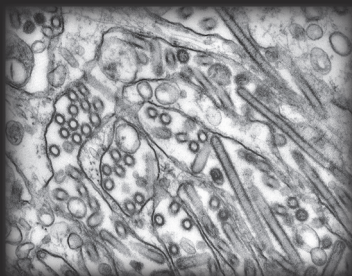
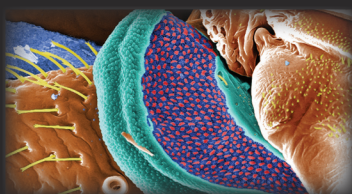
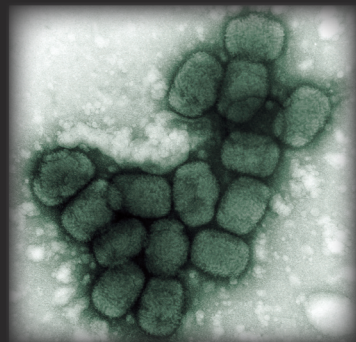
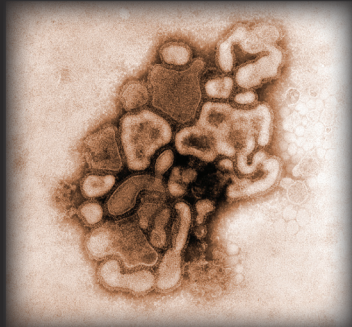
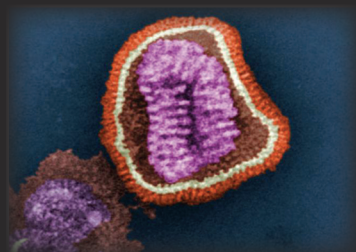
References

- Gao R, Cao B, Hu Y, Feng Z, Wang D, Hu W, et al. Human infection with a novel avian-origin influenza A (H7N9) virus. *N Engl J Med*. 2013;368:1888–97. <http://dx.doi.org/10.1056/NEJMoa1304459e>
- Su S, Gu M, Liu D, Cui J, Gao GF, Zhou J, et al. Epidemiology, evolution, and pathogenesis of H7N9 influenza viruses in five epidemic waves since 2013 in China. *Trends Microbiol*. 2017;25:713–28. <http://dx.doi.org/10.1016/j.tim.2017.06.008>
- Zhang F, Bi Y, Wang J, Wong G, Shi W, Hu F, et al. Human infections with recently-emerging highly pathogenic H7N9 avian influenza virus in China. *J Infect*. 2017;75:71–5. <http://dx.doi.org/10.1016/j.jinf.2017.04.001>
- Zhu W, Zhou J, Li Z, Yang L, Li X, Huang W, et al. Biological characterisation of the emerged highly pathogenic avian influenza (HPAI) A(H7N9) viruses in humans, in mainland China, 2016 to 2017. *Euro Surveill*. 2017;22: pii:30533. <http://dx.doi.org/10.2807/1560-7917.ES.2017.22.19.30533>

5. Ke C, Mok CKP, Zhu W, Zhou H, He J, Guan W, et al. Human infection with highly pathogenic avian influenza A(H7N9) virus, China. *Emerg Infect Dis*. 2017;23:1332–40. <http://dx.doi.org/10.3201/eid2308.170600>
6. Imai M, Watanabe T, Kiso M, Nakajima N, Yamayoshi S, Iwatsuki-Horimoto K, et al. A highly pathogenic avian H7N9 influenza virus isolated from a human is lethal in some ferrets infected via respiratory droplets. *Cell Host Microbe*. 2017;22:615–26.e8. <http://dx.doi.org/10.1016/j.chom.2017.09.008>
7. Yamayoshi S, Yamada S, Fukuyama S, Murakami S, Zhao D, Uraki R, et al. Virulence-affecting amino acid changes in the PA protein of H7N9 influenza A viruses. *J Virol*. 2014;88:3127–34. <http://dx.doi.org/10.1128/JVI.03155-13>
8. Yamayoshi S, Fukuyama S, Yamada S, Zhao D, Murakami S, Uraki R, et al. Amino acids substitutions in the PB2 protein of H7N9 influenza A viruses are important for virulence in mammalian hosts. *Sci Rep*. 2015;5:8039. <http://dx.doi.org/10.1038/srep08039>
9. Xiao C, Ma W, Sun N, Huang L, Li Y, Zeng Z, et al. PB2-588 V promotes the mammalian adaptation of H10N8, H7N9 and H9N2 avian influenza viruses. *Sci Rep*. 2016;6:19474. <http://dx.doi.org/10.1038/srep19474>
10. Mänz B, de Graaf M, Mögling R, Richard M, Bestebroer TM, Rimmelzwaan GF, et al. Multiple natural substitutions in avian influenza A virus PB2 facilitate efficient replication in human cells. *J Virol*. 2016;90:5928–38. <http://dx.doi.org/10.1128/JVI.00130-16>
11. Mok CK, Lee HH, Lestra M, Nicholls JM, Chan MC, Sia SF, et al. Amino acid substitutions in polymerase basic protein 2 gene contribute to the pathogenicity of the novel A/H7N9 influenza virus in mammalian hosts. *J Virol*. 2014;88:3568–76. <http://dx.doi.org/10.1128/JVI.02740-13>
12. Li Y, Qi W, Qiao J, Chen C, Liao M, Xiao C. Evolving HA and PB2 genes of influenza A (H7N9) viruses in the fifth wave—increasing threat to both birds and humans? *J Infect*. 2017;75:184–6. <http://dx.doi.org/10.1016/j.jinf.2017.04.002>
13. Mukaigawa J, Nayak DP. Two signals mediate nuclear localization of influenza virus (A/WSN/33) polymerase basic protein 2. *J Virol*. 1991;65:245–53.
14. Huarte M, Sanz-Ezquerro JJ, Roncal F, Ortín J, Nieto A. PA subunit from influenza virus polymerase complex interacts with a cellular protein with homology to a family of transcriptional activators. *J Virol*. 2001;75:8597–604. <http://dx.doi.org/10.1128/JVI.75.18.8597-8604.2001>
15. Long JS, Giotis ES, Moncorgé O, Frise R, Mistry B, James J, et al. Species difference in ANP32A underlies influenza A virus polymerase host restriction. *Nature*. 2016;529:101–4. <http://dx.doi.org/10.1038/nature16474>

Address for correspondence: Yoshihiro Kawaoka, Division of Virology, Department of Microbiology and Immunology, Institute of Medical Science, University of Tokyo, Minato-ku, Tokyo 108-8639, Japan; email: yoshihiro.kawaoka@wisc.edu or yamayo@ims.u-tokyo.ac.jp

The Public Health Image Library (PHIL)



The Public Health Image Library (PHIL), Centers for Disease Control and Prevention, contains thousands of public health–related images, including high-resolution (print-quality) photographs, illustrations, and videos.

PHIL collections illustrate current events and articles, supply visual content for health promotion brochures, document the effects of disease, and enhance instructional media.

PHIL images, accessible to PC and Macintosh users, are in the public domain and available without charge.

Visit PHIL at <http://phil.cdc.gov/phil>

Enhanced Replication of Highly Pathogenic Influenza A(H7N9) Virus in Humans

Technical Appendix

Additional Methods and Details

Ethics and biosafety statements. All experiments with H5N1 and H7N9 viruses were performed in biosafety level 3 (BSL3) laboratories at the University of Tokyo, which were approved for such use by the Ministry of Agriculture, Forestry, and Fisheries, Japan. All experiments with mice were performed in accordance with the University of Tokyo's Regulations for Animal Care and Use and were approved by the Animal Experiment Committee of the Institute of Medical Science, the University of Tokyo.

Cells. Madin-Darby canine kidney (MDCK) cells were maintained in Eagle's minimal essential medium (MEM) containing 5% newborn calf serum (NCS). Human embryonic kidney 293T cells and chicken fibroblast DF-1 cells were maintained in Dulbecco's modified Eagle's medium (DMEM) containing 10% fetal calf serum (FCS). Human alveolar adenocarcinoma epithelial A549 cells were maintained in Ham's F12-K containing 10% FCS. MDCK, 293T, and A549 cells were maintained at 37°C under 5% CO₂. DF-1 cells were maintained at 39°C under 5% CO₂.

Plasmids. Viral RNA expression plasmids (pHH21) encoding each of the eight virus segments and protein expression plasmids (pCAGGS) encoding PB2, PB1, PA, and NP derived from A/Anhui/1/2013 (H7N9; AN) or A/Guangdong/17SF003/2016 (H7N9; GD) were

previously described (1). Plasmids encoding PB2 mutants of A/Anhui/1/2013 (AN/PB2–627E and AN/PB2–627E-701N) were also described previously (1).

Mutations in the PB2 and PA genes were generated by PCR amplification of the RNA polymerase I plasmid for the PB2 and PA segments with primers possessing the desired mutations (primer sequences available upon request). The PCR products were cloned into pHH21 or pCAGGS/MCS. All constructs were sequenced to confirm the absence of unwanted mutations.

Minigenome assay. A minigenome assay based on the dual-luciferase system was performed as previously reported (2,3). Briefly, human A549 and chicken DF-1 cells were transfected with viral protein expression plasmids for NP, PB1, PB2 or its mutants, and PA or its mutants (0.2 µg each), with a plasmid expressing a reporter vRNA encoding the firefly luciferase gene under the control of the human or chicken RNA polymerase I promoter (pPolI/NP(0)Fluc(0) or pPolIGG-NP(0)Fluc(0), respectively, 0.2 µg each), and pRL null (Promega, 0.2 µg), which expresses Renilla luciferase, as a transfection control. The luciferase activities in the A549 cells incubated at 33 or 37°C and the DF-1 cells incubated at 39°C were measured by using the Dual-Glo Luciferase Assay System (Promega) at 24 h post-transfection. Polymerase activity was calculated by standardization of the firefly luciferase activity to the Renilla luciferase activity. Relative polymerase activities are presented in the figures.

Reverse genetics. Plasmid-based reverse genetics for virus generation was performed as previously described (4). Briefly, eight RNA polymerase I plasmids (for the synthesis of the eight influenza A viral RNAs) together with plasmids for the expression of the PB2, PB1, PA, and NP proteins derived from the influenza A virus strain A/WSN/33 (H1N1) were transfected into 293T cells. At 24 h post-transfection, culture supernatants were harvested and inoculated

into embryonated chicken eggs for virus propagation. After 1 or 2 days, allantoic fluids containing viruses were collected and centrifuged to remove cell debris and the supernatants were stored as stock viruses. The titers of the stock viruses were determined by means of plaque assays in MDCK cells. All viruses were sequenced to confirm the absence of unwanted mutations.

Growth kinetics of viruses in cell culture. The growth kinetics of the viruses was assessed as previously described (1). Briefly, A549 and DF-1 cells were infected with the indicated viruses at a multiplicity of infection (MOI) of 0.001. After incubation at 37°C for 1 h, the viral inoculum was replaced with MEM containing 0.3% bovine serum albumin and TPCK-treated trypsin (0.3 µg/ml), followed by further incubation at 33 or 37°C for A549 cells or 39°C for DF-1 cells. Cell culture supernatants were collected at 24, 48, and 72 h post-infection and subjected to virus titration by use of plaque assays in MDCK cells.

Experimental infection of mice. Baseline bodyweights of all mice were measured before infection. Five 6-week-old female BALB/c mice (Japan SLC) per group were intranasally inoculated with 10^2 – 10^5 PFUs (PFU) (in 50 µl) of the indicated viruses under anesthesia. Bodyweight and survival were monitored daily for 14 days; mice with bodyweight loss of more than 25% of their baseline bodyweight were euthanized. For virologic examinations, six mice per group were intranasally infected with 10^2 PFU (in 50 µl) of the viruses and three mice per group were euthanized at 3 and 6 days post-infection. The virus titers in the nasal turbinate, lung, and brain were determined by means of plaque assays in MDCK cells.

Phylogenetic analysis. The phylogenetic tree of the HA nucleotide sequences derived from the H7N9 viruses was constructed by using the neighbor-joining (NJ) method with the Kimura distances and the bootstrap procedure (n = 1000) using ClustalW 2.1 on the DDBJ

(DNA Data Bank of Japan) Web site (<http://clustalw.ddbj.nig.ac.jp/>) and was visualized by using the MEGA 7.0 software. Sequence data for HA, PB2, and PA were obtained from GISAID databases on August 31, 2017. The sequencing dataset used in this study is available upon request.

Molecular modeling. The structural model of the polymerase complex derived from A/little yellow-shouldered bat/Guatemala/060/2010 (H17N10) (PDB code, 4WSB) was used to assign the amino acid positions in the influenza A virus polymerase complex with the PyMOL Molecular Graphics System, version 1.3.

References

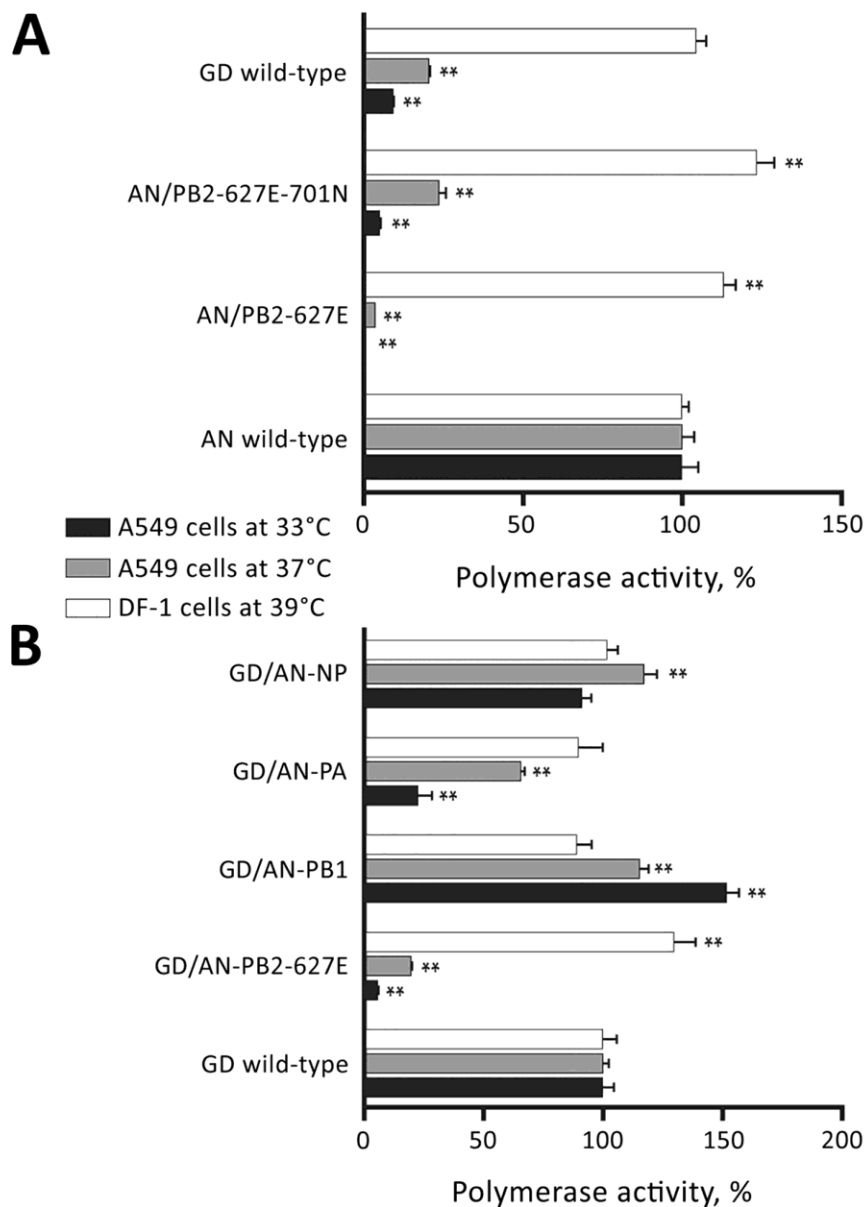
1. Yamayoshi S, Fukuyama S, Yamada S, Zhao D, Murakami S, Uraki R, et al. Amino acids substitutions in the PB2 protein of H7N9 influenza A viruses are important for virulence in mammalian hosts. *Sci Rep.* 2015;5:8039. [PubMed http://dx.doi.org/10.1038/srep08039](http://dx.doi.org/10.1038/srep08039)
2. Yamayoshi S, Yamada S, Fukuyama S, Murakami S, Zhao D, Uraki R, et al. Virulence-affecting amino acid changes in the PA protein of H7N9 influenza A viruses. *J Virol.* 2014;88:3127–34. [PubMed http://dx.doi.org/10.1128/JVI.03155-13](http://dx.doi.org/10.1128/JVI.03155-13)
3. Imai M, Watanabe T, Kiso M, Nakajima N, Yamayoshi S, Iwatsuki-Horimoto K, et al. A Highly Pathogenic Avian H7N9 Influenza Virus Isolated from A Human Is Lethal in Some Ferrets Infected via Respiratory Droplets. *Cell host & microbe.* 2017 Nov 8;22(5):615–26 e8.
4. Neumann G, Watanabe T, Ito H, Watanabe S, Goto H, Gao P, et al. Generation of influenza A viruses entirely from cloned cDNAs. *Proc Natl Acad Sci U S A.* 1999;96:9345–50. [PubMed http://dx.doi.org/10.1073/pnas.96.16.9345](http://dx.doi.org/10.1073/pnas.96.16.9345)

Technical Appendix Table. Percentage of isolates with the indicated amino acid residue at each position*

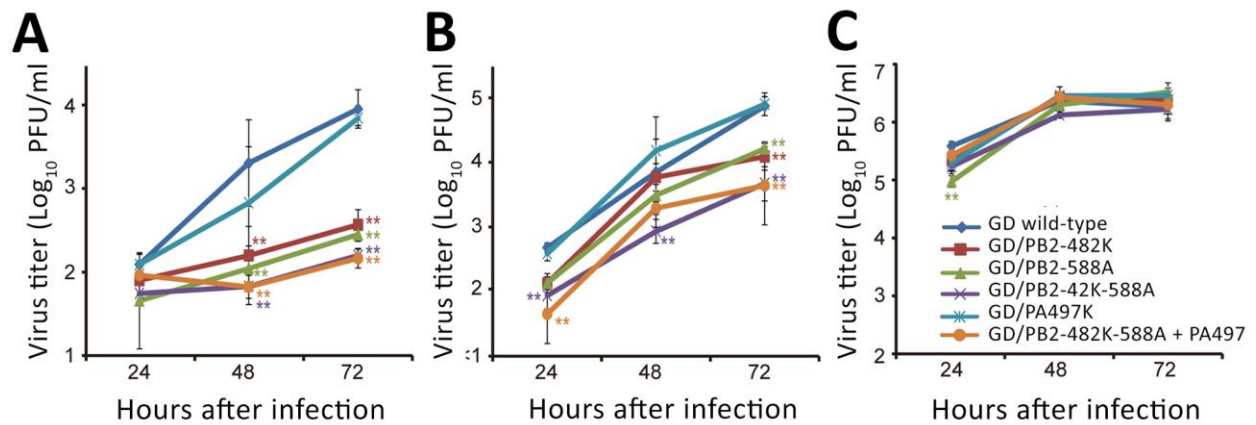
Subtype	Host	PB2						PA	
		482		588				497	
		K	R†	A	T	I	V†	K	R†
Pre2009 H1N1	Human	99.9	0.11	0.89	0.33	97.8	0.9	99.9	0
H1N1pdm09	Human	99.8	0.2	0.08	97.3	0.26	0	99.9	0.05
H3N2	Human	99.9	0.04	0.04	29.5	68.5	1.8	98.7	1.29
H5N1	Human	100	0	93.7	5.93	0.37	0	94.1	5.92
H7N9	Human	99.2	0.79	82.9	0.34	0.11	16.6	98.2	0.81
H1N1	Swine	99.1	0.84	38.0	55.6	3.66	0.92	94.4	5.5
H1N2	Swine	98.6	1.45	19.2	74.7	4.92	0.72	79.3	20.5
H3N2	Swine	98.6	1.2	6.73	85.1	6.73	0.98	68.7	31.4
H5N1	Avian	100	0	93.7	5.93	0.37	0	94.1	5.9
H7N9	Avian	100	0	93.3	0	0.32	6.39	100	0
Other (i.e., not H5N1 or H7N9)	Avian	99.5	0.43	92.3	3.26	0.59	3.72	99.3	0.66

*The percentages are based on inspection of ≈900, 3830, 7590, 270, 870, 1310, 690, 920, 270, 310, and 6780 sequences of PB2 or PA derived from human pre2009 H1N1, H1N1pdm09, H3N2, H5N1, H7N9, swine H1N1, H1N2, H3N2, avian H5N1, H7N9, and other virus subtypes, respectively.

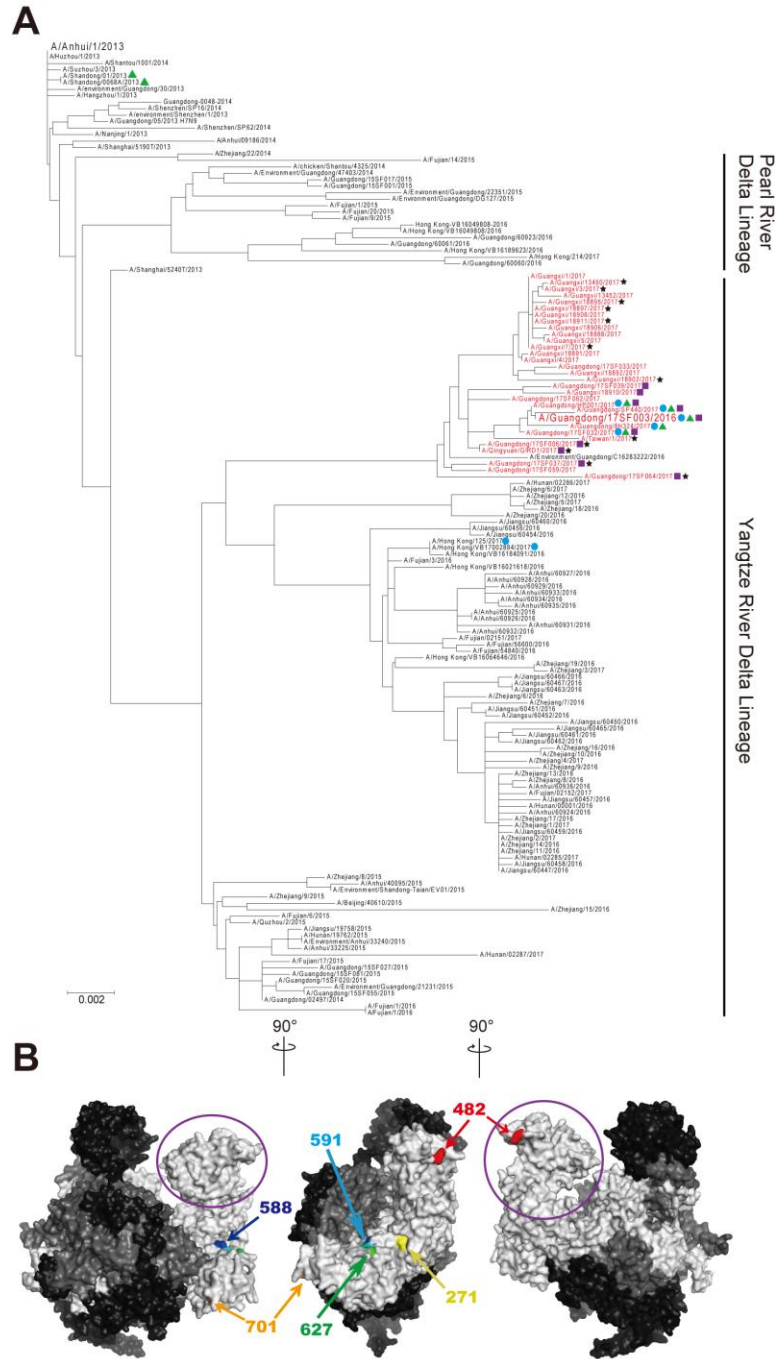
†Residues involved in enhanced replication are shown in boldface.



Technical Appendix Figure 1. Each GD-PB2 and -PA is required for enhanced viral polymerase activity in human cells. Viral polymerase activity of wild-type AN, AN-PB2 mutants, and wild-type GD (A) or wild-type and reassortant GD (B) polymerase complex in human A549 and avian DF-1 cells. The viral polymerase activity AN wild-type (A) or GD wild-type (B) was set to 100%. The data shown are relative viral polymerase activities \pm SD (n = 3). **p < 0.01, according to a one-way ANOVA followed by a Dunnett's test.



Technical Appendix Figure 2. Growth kinetics of wild-type and mutant GD viruses in human and avian cells. Human A549 cells and chicken DF-1 cells were infected with the wild-type or indicated mutant viruses at an MOI of 0.001 and incubated at 33°C (A) or 37°C (B) for A549 cells and 39°C for DF-1 cells (C). The culture media from the infected cells was collected at the indicated time points. Virus titers were determined by use of a plaque assay in MDCK cells. The average virus titers \pm SD are plotted (n = 3). **p < 0.01, according to a two-way analysis of variance (ANOVA) followed by a Dunnett's test.



Technical Appendix Figure 3. Phylogenetic and structural position of PB2–482R and PA-497R. (A)

Phylogenetic tree based on H7N9 HA sequences. Virus isolates marked by cyan circles or green triangles possess PB2–482R or PA-497R, respectively. Highly pathogenic isolates marked by purple squares or black stars possess PB2–588V or PB2–627K, respectively. Red letters indicate highly pathogenic

isolates. (B) Localization of the mammalian adaptive amino acids in the polymerase complex. The polymerase subunits PB2, PB1, and PA are shown as white, gray, and black, respectively. Each amino acid (PB2-271A, PB2-482R, PB2-588V, PB2-591K, PB2-627K, and PB2-701N) of PB2 that is involved in enhanced replication in mammalian hosts is mapped on the structure. PA-497R is not exposed on the molecular surface of this model. The cap binding domain is indicated by purple circles.